



TEST OF PARAMETRIZED POST-NEWTONIAN GRAVITY WITH GALAXY-SCALE STRONG LENSING SYSTEMS

SHUO CAO¹, XIAOLEI LI¹, MAREK BIESIADA^{1,2}, TENGPENG XU¹, YONGZHI CAI¹, AND ZONG-HONG ZHU¹

¹Department of Astronomy, Beijing Normal University, 100875, Beijing, China; zhuzh@bnu.edu.cn

²Department of Astrophysics and Cosmology, Institute of Physics, University of Silesia, Uniwersytecka 4, 40-007 Katowice, Poland
Received 2016 September 11; revised 2016 November 18; accepted 2016 December 2; published 2017 January 20

ABSTRACT

Based on a mass-selected sample of galaxy-scale strong gravitational lenses from the SLACS, BELLS, LSD, and SL2S surveys and using a well-motivated fiducial set of lens-galaxy parameters, we tested the weak-field metric on kiloparsec scales and found a constraint on the post-Newtonian parameter $\gamma = 0.995^{+0.037}_{-0.047}$ under the assumption of a flat Λ CDM universe with parameters taken from *Planck* observations. General relativity (GR) predicts exactly $\gamma = 1$. Uncertainties concerning the total mass density profile, anisotropy of the velocity dispersion, and the shape of the light profile combine to systematic uncertainties of $\sim 25\%$. By applying a cosmological model-independent method to the simulated future LSST data, we found a significant degeneracy between the PPN γ parameter and the spatial curvature of the universe. Setting a prior on the cosmic curvature parameter $-0.007 < \Omega_k < 0.006$, we obtained the constraint on the PPN parameter that $\gamma = 1.000^{+0.0023}_{-0.0025}$. We conclude that strong lensing systems with measured stellar velocity dispersions may serve as another important probe to investigate validity of the GR, if the mass-dynamical structure of the lensing galaxies is accurately constrained in future lens surveys.

Key words: galaxies: structure – gravitational lensing: strong – cosmology: observations

1. INTRODUCTION

As a successful geometric theory of gravitation, Einstein's theory of general relativity (GR) has been confirmed in all observations devoted to its testing to date (Ashby 2002; Bertotti et al. 2003), in particular in some famous experiments (Dyson et al. 1920; Pound & Rebka 1960; Shapiro 1964; Taylor et al. 1979). However, the pursuit of testing gravity at a much higher precision has continued in recent decades, including measurements of the Earth–moon separation as a function of time through lunar laser ranging (Williams et al. 2004). On the other hand, formulating and quantitatively interpreting the test of gravity is another question; an interesting proposal, in this respect, has been formulated in the frameworks of the parameterized post-Newtonian (PPN) framework (Thorne & Will 1971). Different from the original physical indication (Bertotti et al. 2003), the scale-independent post-Newtonian parameter denoted by γ , with $\gamma = 1$ representing GR, may serve as a test of the theory on large distances.

This paper is focused on the quantitative constraints of GR as a theory of gravity, using the recently released large sample of galaxy-scale strong gravitational lensing systems discovered and observed in SLACS, BELLS, LSD, and SL2S surveys (Cao et al. 2015a). Up until now, most of the progress in strong gravitational lensing has been made in investigating cosmological parameters (Zhu 2000a, 2000b; Chae 2003; Chae et al. 2004; Mitchell et al. 2005; Biesiada 2006; Grillo et al. 2008; Oguri et al. 2008; Zhu & Sereno 2008; Zhu et al. 2008; Biesiada et al. 2010; Cao & Zhu 2012; Cao et al. 2012a, 2012b, 2012c; Collett & Auger 2014; Bonvin et al. 2016; Cardone et al. 2016), the distribution of matter in massive galaxies acting as lenses (Zhu & Wu 1997; Mao & Schneider 1998; Jin et al. 2000; Keeton 2001; Ofek et al. 2003; Treu et al. 2006), and the photometric properties of background sources at cosmological distances (Cao et al. 2015b). All of the above-mentioned results have been obtained under the assumption that GR is valid. Using strong lensing systems, Grillo et al. (2008) reported the value for the present-day matter

density Ω_m ranging from 0.2 to 0.3 at a 99% confidence level. This initial result, confirmed in later strong lensing studies (e.g., Cao et al. 2012b, 2015a), is consistent with most current data, including precision measurements of Type Ia supernovae (Amanullah et al. 2010) and anisotropies in the cosmic microwave background radiation (Ade et al. 2014). Currently, the concordance Λ CDM model is in agreement with most available cosmological observations in which the cosmological constant contributing more than 70% of the total energy of the universe is playing the role of an exotic component, called dark energy, responsible for the accelerated expansion of the universe. However, there appear to be noticeable tensions between different cosmological probes. For example, regarding H_0 , there is a tension between the CMB results from Planck (Ade et al. 2014) and the most recent Type Ia supernovae data (Riess et al. 2016). Similarly, the σ_8 parameter derived from the CMB results from Planck (Ade et al. 2014) turned out to be in tension with recent tomographic cosmic shear results both from the Canada–France–Hawaii Telescope Lensing Survey (CFHTLenS; Heymans et al. 2012; MacCrann et al. 2015) and the Kilo Degree Survey (KiDS; Hildebrandt et al. 2016). These tensions partly motivate the test of GR performed in the present paper.

With reasonable prior assumptions and independent measurements concerning background cosmology and internal structure of lensing galaxies, one can use strong lensing systems as another tool to constrain the PPN parameters describing the deviations from GR. This idea was first adopted on 15 SLACS lenses by Bolton et al. (2006), who found the post-Newtonian parameter to be $\gamma = 0.98 \pm 0.07$ based on priors on galaxy structure from local observations. More recently, Schwab et al. (2010) re-examined the expanded SLACS sample (Bolton et al. 2008) and obtained a constraint on the PPN parameter $\gamma = 1.01 \pm 0.05$.

Having available reasonable catalogs of strong lenses that contain more than 100 lenses, with spectroscopic as well as astrometric data obtained with well-defined selection criteria

(Cao et al. 2015a), the purpose of this work is to use a mass-selected sample of 80 early-type lenses compiled from SLACS, BELLS, LSD, and SL2S to provide independent constraints on the post-Newtonian parameter γ . Throughout this paper we assume a flat Λ CDM cosmology with parameters based on the recent *Planck* observations (Ade et al. 2014).

2. METHOD AND DATA

Our goal will be to constrain deviations from general relativity at the level of γ post-Newtonian parameter. The PPN form of the Schwarzschild metric can be written as

$$d\tau^2 = c^2 dt^2 (1 - 2GM/c^2 r) - dr^2 (1 - 2\gamma GM/c^2 r) - r^2 d\Omega^2, \quad (1)$$

where general relativity corresponds to $\gamma = 1$.

From the theory of gravitational lensing (Schneider et al. 1992), for a specific strong lensing system with the intervening galaxy acting as a lens, multiple images can form with angular separations close to the so-called Einstein radius θ_E :

$$\theta_E = \sqrt{\frac{1 + \gamma}{2}} \left(\frac{4GM_E}{c^2} \frac{D_{ls}}{D_s D_l} \right)^{1/2}, \quad (2)$$

where M_E is the mass enclosed within a cylinder of radius equal to the Einstein radius, D_s is the distance to the source, D_l is the distance to the lens, and D_{ls} is the distance between the lens and the source. All the above-mentioned distances are angular diameter distances. Rearranging terms with $R_E = D_l \theta_E$ (R is the cylindrical radius perpendicular to the line of sight—the Z -axis), we obtain a useful formula:

$$\frac{GM_E}{R_E} = \frac{2}{(1 + \gamma)} \frac{c^2}{4} \frac{D_s}{D_{ls}} \theta_E, \quad (3)$$

which indicates that only the matter within the Einstein ring is important according to the Gauss's law.

On the other hand, spectroscopic measurements of central velocity dispersions σ in elliptical galaxies can provide a dynamical estimate of this mass based on power-law density profiles for the total mass density, ρ , and luminosity density, ν (Koopmans 2006):

$$\rho(r) = \rho_0 \left(\frac{r}{r_0} \right)^{-\alpha} \quad (4)$$

$$\nu(r) = \nu_0 \left(\frac{r}{r_0} \right)^{-\delta}. \quad (5)$$

Here, r is the spherical radial coordinate from the lens center, $r^2 = R^2 + Z^2$. In order to characterize anisotropic distribution of the three-dimensional velocity dispersion pattern, one introduces (Bolton et al. 2006; Koopmans 2006) an anisotropy parameter β ,

$$\beta(r) = 1 - \sigma_t^2 / \sigma_r^2, \quad (6)$$

where σ_t^2 and σ_r^2 are, respectively, the tangential and radial components of the velocity dispersion. In the current analysis, we will consider anisotropic distribution $\beta \neq 0$ and assume, as it almost always is assumed, that β is independent of r .

Following the well-known spherical Jeans equation (Binney 1980), the radial velocity dispersion of the luminous matter $\sigma_r^2(r)$ in the early-type lens galaxies can be expressed as

$$\sigma_r^2(r) = \frac{G \int_r^\infty dr' \nu(r') M(r') (r')^{2\beta-2}}{r^{2\beta} \nu(r)}, \quad (7)$$

where β is a constant velocity anisotropy parameter. Combining the mass density profiles in Equation (4), we obtain the relation between the mass enclosed within a spherical radius r and M_E as

$$M(r) = \frac{2}{\sqrt{\pi} \lambda(\alpha)} \left(\frac{r}{R_E} \right)^{3-\alpha} M_E, \quad (8)$$

where by $\lambda(x) = \Gamma\left(\frac{x-1}{2}\right) / \Gamma\left(\frac{x}{2}\right)$ we denoted the ratio of respective Euler's Gamma functions. Simplifying the formulae with the notation $\xi = \delta + \alpha - 2$ taken after Koopmans (2006), we obtain a convenient form for the radial velocity dispersion by scaling the dynamical mass to the Einstein radius:

$$\sigma_r^2(r) = \left[\frac{GM_E}{R_E} \right] \frac{2}{\sqrt{\pi} (\xi - 2\beta) \lambda(\alpha)} \left(\frac{r}{R_E} \right)^{2-\alpha}. \quad (9)$$

In all strong lensing measurements used, the *observed* velocity dispersion is reported, which is a projected luminosity-weighted average of the radially dependent velocity dispersion profile of the lensing galaxy. Its theoretical value can be calculated from Equation (7) with the assumption that the relationship between stellar number density and stellar luminosity density is spatially constant. This assumption is unlikely to be violated appreciably within the effective radius of the early-type lens galaxies under consideration.

Moreover, the actual observed velocity dispersion is measured over the effective spectrometer aperture θ_{ap} and effectively averaged by line-of-sight luminosity. Taking into account the effects of aperture with atmospheric blurring and luminosity-weighted averaging, the averaged observed velocity dispersion takes the form

$$\begin{aligned} \bar{\sigma}_*^2 = & \left[\frac{c^2}{4} \frac{D_s}{D_{ls}} \theta_E \right] \frac{2}{\sqrt{\pi}} \frac{(2\tilde{\sigma}_{\text{atm}}^2 / \theta_E^2)^{1-\alpha/2}}{(\xi - 2\beta)} \\ & \times \left[\frac{\lambda(\xi) - \beta \lambda(\xi + 2)}{\lambda(\alpha) \lambda(\delta)} \right] \frac{\Gamma\left(\frac{3-\xi}{2}\right)}{\Gamma\left(\frac{3-\delta}{2}\right)}, \end{aligned} \quad (10)$$

where $\tilde{\sigma}_{\text{atm}} \approx \sigma_{\text{atm}} \sqrt{1 + \chi^2/4 + \chi^4/40}$ and $\chi = \theta_{ap} / \sigma_{\text{atm}}$ (Schwab et al. 2010); σ_{atm} is the seeing recorded by the spectroscopic guide cameras during observing sessions (Cao et al. 2016). The above equation tells us that we can constrain the PPN parameter γ on a sample of lenses with known redshifts of the lens and the source with a measured velocity dispersion and the Einstein radius, provided we have reliable knowledge about the cosmological model and the parameters describing the mass distribution of lensing galaxies (α , β , δ).

For the purpose of our analysis, the angular diameter distances $D_A(z)$ between redshifts z_1 and z_2 were calculated using the best-fit matter density parameter Ω_m given by the *Planck* Collaboration assuming a flat FRW metric (Ade et al. 2014). Moreover, we allow the luminosity density profile to differ from the total mass density profile, i.e., $\alpha \neq \delta$, and the

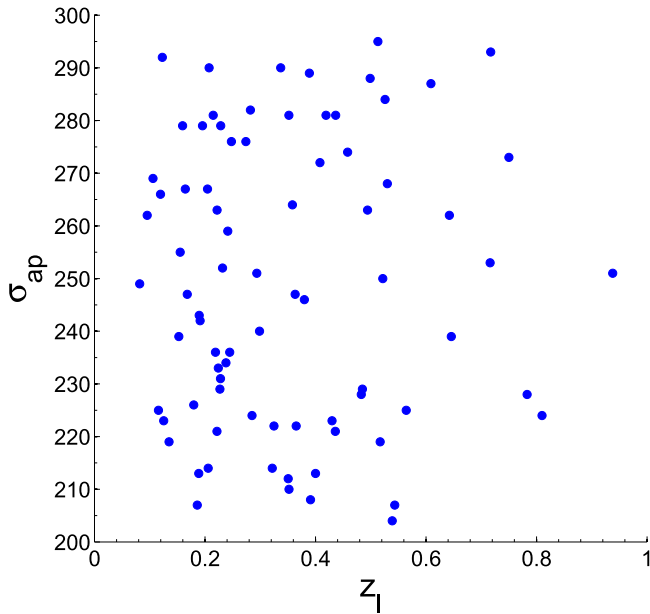


Figure 1. Characteristics of the strong lensing data sample of 80 intermediate-mass early-type galaxies. Observed velocity dispersion inside the aperture is plotted against redshift to the lens.

stellar velocity anisotropy exists, i.e., $\beta \neq 0$. Based on a well-studied sample of nearby elliptical galaxies from Gerhard et al. (2001), the anisotropy β is characterized by a Gaussian distribution, $\beta = 0.18 \pm 0.13$, that is also extensively used in previous works (Bolton et al. 2006; Schwab et al. 2010). More recently, Xu et al. (2016) measured the stellar velocity anisotropy parameter β and its correlations with redshifts and stellar velocity dispersion, based on the Illustris simulated early-type galaxies with spherically symmetric density distributions. It is worth noting from their results that β markedly depends on stellar velocity dispersion and its mean value varies from 0.10 to 0.30 for intermediate-mass galaxies ($200 \text{ km s}^{-1} < \sigma_{ap} \leq 300 \text{ km s}^{-1}$), which is consistent with the values used in our analysis.

Following our previous analysis (Cao et al. 2016) concerning power-law mass and luminosity density profiles of elliptical galaxies, we used a mass-selected sample of strong lensing systems taken from a comprehensive compilation of strong lensing systems observed by four surveys: SLACS, BELLS, LSD, and SL2S. The sample has been defined by restricting the velocity dispersions of lensing galaxies to the intermediate range: $200 \text{ km s}^{-1} < \sigma_{ap} \leq 300 \text{ km s}^{-1}$. Lenses of this subsample are located at redshifts ranging from $z_l = 0.08$ to $z_l = 0.94$. Original data about these strong lenses were derived by Bolton et al. (2008), Auger et al. (2009), Brownstein et al. (2012), Koopmans & Treu (2002), Treu & Koopmans (2002, 2004), and Sonnenfeld et al. (2013a, 2013b), and more comprehensive data concerning these systems can be found in Table 1 of Cao et al. (2015a). Figure 1 shows the scatter plot for this sample in the plane spanned by the redshift of the lens and its velocity dispersion.

3. MAIN RESULTS

Because α and δ could not be independently measured for each lensing galaxy, we first treated them as free parameters and inferred α , δ , and γ simultaneously. Performing fits on the strong lensing data set, the 68% confidence level uncertainties

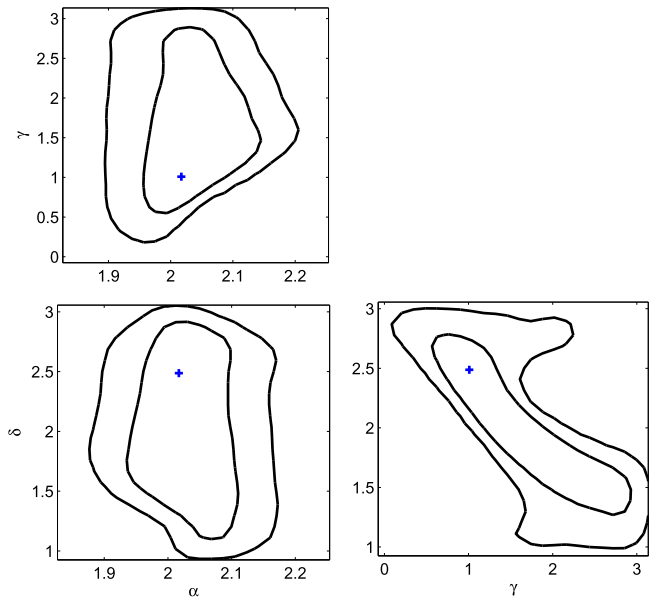


Figure 2. Constraints on the PPN γ parameter, the total mass and luminosity density parameters obtained from the sample of strong lensing systems. Blue crosses denote the best-fit values.

on the three model parameters are

$$\begin{aligned} \alpha &= 2.017^{+0.093}_{-0.082}, \\ \delta &= 2.485^{+0.445}_{-1.393}, \\ \gamma &= 1.010^{+1.925}_{-0.452}. \end{aligned}$$

Figure 2 shows these constraints in the parameter space of α , δ , and γ . It is obvious that the fits on α and δ are consistent with the analysis results of Bolton et al. (2006), Grillo et al. (2008), and Schwab et al. (2010), which are characterized by Gaussian distributions

$$\begin{aligned} \langle \alpha \rangle &= 2.00; \sigma_\alpha = 0.08 \\ \langle \delta \rangle &= 2.40; \sigma_\delta = 0.11. \end{aligned} \quad (11)$$

More importantly, the degeneracy between the two parameters γ and δ is apparently indicated by the results presented in Figure 2, i.e., a steeper luminosity density profile for lensing early-type galaxies will lead to a larger value for the parameterized post-Newtonian parameter. This tendency could also be seen from the sensitivity analysis shown below.

Now the parameters characterizing the total mass-profile shape, velocity anisotropy, and light-profile shape of lenses are set at their best measured values. Performing fits on γ , we find the resulting posterior probability density shown in Figure 3. The result $\gamma = 0.995^{+0.037}_{-0.047}$ (1σ confidence) is consistent with $\gamma = 1$ and also with previous results of Bolton et al. (2006) obtained with strong lensing systems. The scatter of galaxy structure parameters is an important source of systematic errors on the final result. Taking the best-fitted values of the structure parameters as our fiducial model, we investigated how the PPN constraint is altered by introducing the uncertainties on α , β , and δ as listed in Equation (11). Therefore, first, we perform a sensitivity analysis, varying the parameter of interest while fixing the other parameters at their best-fit values. In general, one can see from Table 1 and Figure 4 that the constraint on γ is quite sensitive to small systematic shifts in the adopted lens-galaxy parameters. By comparing the contribution of each of

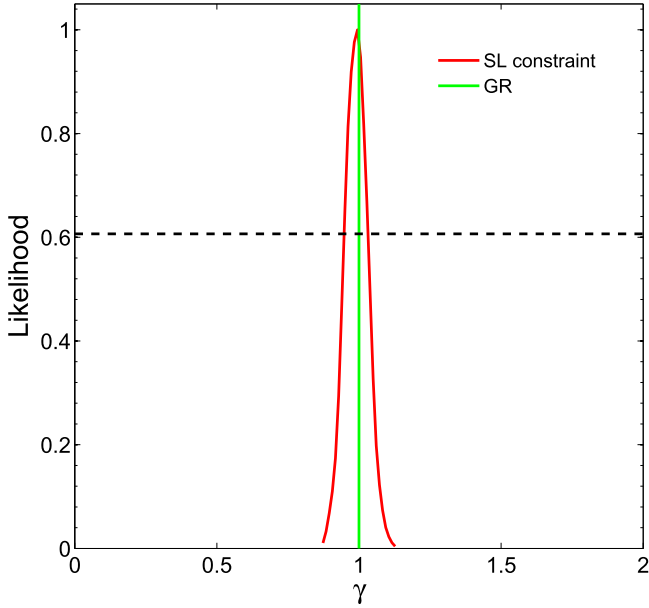


Figure 3. Normalized posterior likelihood of the PPN γ parameter obtained with rigid priors on the nuisance parameters (α , β , δ).

Table 1

Sensitivity of Constraints on γ with Respect to the Galaxy Structure Parameters

Systematics	PPN Parameter
$\alpha = 2.00; \beta = 0.18; \delta = 2.40$	$\gamma = 0.995^{+0.037}_{-0.047}$
$\alpha = 1.92; \beta = 0.18; \delta = 2.40$	$\gamma = 0.860 \pm 0.040$
$\alpha = 2.08; \beta = 0.18; \delta = 2.40$	$\gamma = 1.169 \pm 0.050$
$\alpha = 2.00; \beta = 0.05; \delta = 2.40$	$\gamma = 0.914 \pm 0.043$
$\alpha = 2.00; \beta = 0.31; \delta = 2.40$	$\gamma = 1.087 \pm 0.043$
$\alpha = 2.00; \beta = 0.18; \delta = 2.29$	$\gamma = 1.111 \pm 0.044$
$\alpha = 2.00; \beta = 0.18; \delta = 2.51$	$\gamma = 0.883 \pm 0.039$

these systematic errors to the systematic error on γ , we find that the largest sources of systematic error are the mass density slope α , followed by the anisotropy parameter of velocity dispersion β and the luminosity density slope δ . Second, by taking the intrinsic scatter of α , β , and δ into consideration, we found γ varying from 0.845 to 1.240 at the 1σ confidence level. It means that systematic errors might exceed $\sim 25\%$ of the final result. The large covariances of γ with α and δ seen in Figure 2 motivate the future use of auxiliary data to improve constraints on α , β , and δ . For example, α can be inferred for individual lenses from high-resolution imaging of arcs (Suyu et al. 2007; Vegetti et al. 2010; Collett & Auger 2014; Wong et al. 2015), while constraints on β and δ can be improved with integral field unit (IFU) data (Barnabè et al. 2013), without the assumption of GR.

Another important issue is how much γ is affected by the uncertainty of cosmological parameters of the Λ CDM model used in our study. For this purpose, we also considered the WMAP9 result of $\Omega_m = 0.279$ in order to make a comparison with *Planck* observations. Not surprisingly, results showed that the differences were negligible. This could have been expected, since cosmology intervenes here through the distance ratio D_{ls}/D_s , which is very weakly dependent on the value of Ω_m and in flat cosmology does not depend on H_0 at all.

The next generation of wide and deep sky surveys with improved depth, area, and resolution may, in the near future,

increase the current galactic-scale lens sample sizes by orders of magnitude (Kuhlen et al. 2004; Marshall et al. 2005). Such a significant increase of the number of strong lensing systems will considerably improve the constraints on the PPN parameter. Now we will illustrate what kind of results may be found using future data from the forthcoming Large Synoptic Survey Telescope (LSST) survey, which may detect 120000 lenses for the most optimistic scenario (Collett 2015). In order to make a good comparison with the results derived with current strong lensing systems (Figure 2), we first turn to the simulated LSST population containing ~ 40000 lensing galaxies with intermediate velocity dispersions ($200 \text{ km s}^{-1} < \sigma_{ap} \leq 300 \text{ km s}^{-1}$).³ Performing fits on this simulated strong lensing data set, we obtain the constraints in the parameter space of α , δ , and γ , shown in Figure 5. It is apparent from the simulated LSST strong lensing data that we may expect the total mass density parameter α to be estimated with 10^{-3} precision. However, the degeneracy between the PPN γ parameter and the luminosity density parameter δ still needs to be investigated with future high-quality integral field unit (IFU) data (Barnabè et al. 2013). In the next section, we will apply a cosmological-independent method to study the degeneracy (Räsänen et al. 2015) between cosmic curvature and parameterized post-Newtonian parameter γ .

4. COSMIC CURVATURE AND PARAMETERIZED POST-NEWTONIAN FORMALISM

In a homogeneous and isotropic universe, the dimensionless distance $d(z_l; z_s) = (H_0/c)(1 + z_s)D_A(z_l; z_s)$ can be written as

$$d(z_l; z_s) = \frac{1}{\sqrt{|\Omega_k|}} \text{sinn} \left[\sqrt{|\Omega_k|} \int_{z_l}^{z_s} \frac{dz'}{E(z')} \right], \quad (12)$$

where $E(z) = H(z)/H_0$ is the expansion rate and Ω_k is the spatial curvature density parameter; $\text{sinn}(x) = \sinh(x)$ for $\Omega_k > 0$, $\text{sinn}(x) = x$ for $\Omega_k = 0$, and $\text{sinn}(x) = \sin(x)$ for $\Omega_k < 0$, respectively. For a strong lensing system with the notation $d(z) = d(0; z)$, $d_l = d(0; z_l)$, $d_s = d(0; z_s)$, and $d_{ls} = d(z_l; z_s)$, a simple sum rule could be easily obtained as

$$d_{ls}/d_s = \sqrt{1 + \Omega_k d_l^2} - d_l/d_s \sqrt{1 + \Omega_k d_s^2}. \quad (13)$$

(The case of Equation (13) is given in, e.g., Peebles 1993.) This fundamental formula provides a model-independent probe to test both the spatial curvature, in combination with weak lensing and baryon acoustic oscillations (BAO) measurements (Bernstein 2006), and the FLRW metric, in combination with strong lensing systems and SNe Ia observations (Räsänen et al. 2015).

For the purpose of our analysis, we determined the dimensionless distances d_l and d_s of all “observed” strong lensing systems (taken from the LSST simulation by Collett 2015) by fitting a polynomial to the Union2.1 SN Ia data covering the redshift range $0 < z \leq 1.414$ (Amanullah et al. 2010). Therefore, we bypassed the need to assume any specific cosmological model. By using Equation (13) we were able to calculate the distance ratio d_{ls}/d_s depending only on the curvature density parameter Ω_k . The reported statistical and systematic uncertainties of the distance modulus for individual

³ Our simulated LSST sample is obtained with the simulation programs available on the github.com/tcollett/LensPop.

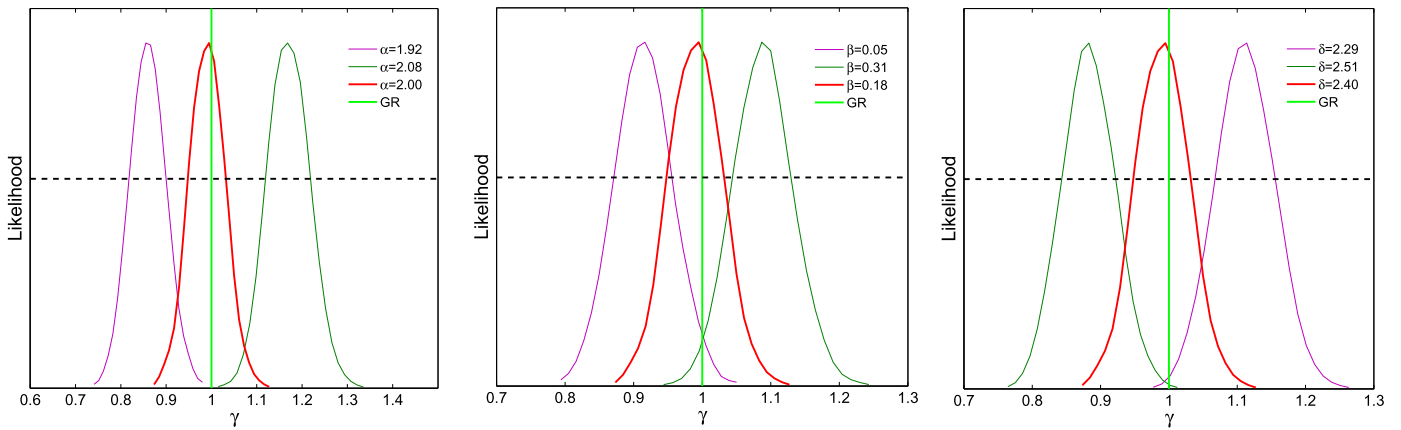


Figure 4. Normalized likelihood plot for γ by choosing different galaxy structure parameters.

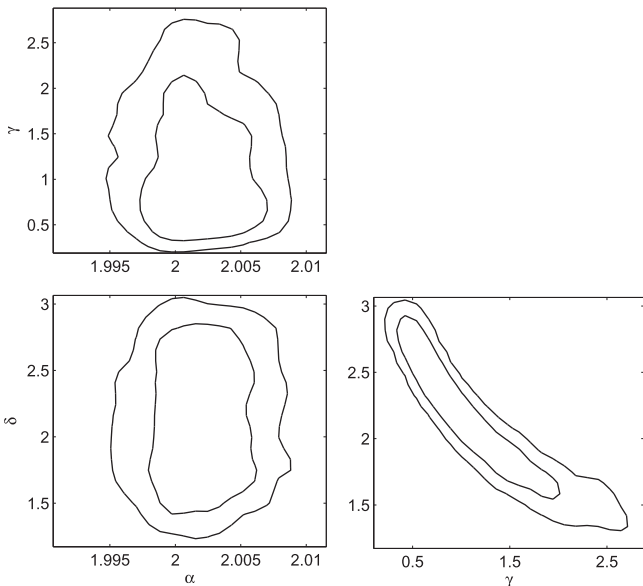


Figure 5. Constraints on the PPN γ parameter, the total mass and luminosity density parameters obtained from the simulated LSST strong lensing data.

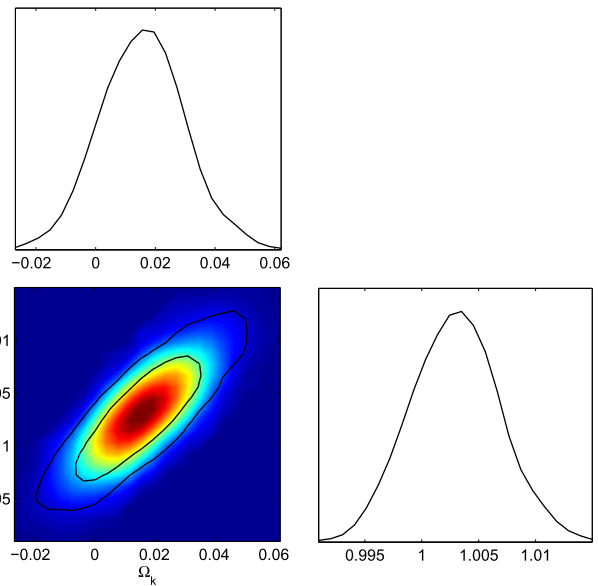


Figure 6. Constraints on the PPN parameter and cosmic curvature from the simulated LSST strong lensing data.

SNe Ia are considered in the fitting procedure. In the Union2.1 SN Ia compilation, light-curve fitting parameters, which are used for distance estimation, are constrained in a global fit. However, compared to the uncertainties in the modeling of the strong lensing systems, the model-dependence of the SNe Ia analysis is likely subdominant (Räsänen et al. 2015). We then assessed the distance ratios d_{ls}/d_s from the strong lensing data (Einstein radius and velocity dispersion) according to Equation (10). For this purpose we used the simulated observations of forthcoming photometric LSST survey (Collett 2015). Using the simulation programs available on github.com/tcollett/LensPop, we obtained 53,000 strong lensing systems meeting the redshift criterion $0 < z_l < z_s \leq 1.414$ in compliance with SN Ia data used in parallel. The simulated catalog is derived on the base of realistic population models of elliptical galaxies acting as lenses, with the mass distribution approximated by the singular isothermal ellipsoids.

Following the assumptions underlying the simulation, we fixed $\alpha = \delta = 2$ and $\beta = 0$ in our analysis. We took the fractional uncertainty of the Einstein radius at a level of 1% and the observed velocity dispersion at a level of 10%. Secondary lensing contribution from the matter along the line

of sight was neglected in our analysis.⁴ Figure 6 displays the fitting results in the $\Omega_k - \gamma$ plane, thus illustrating the dependence between the cosmic curvature and the PPN γ parameter. It is apparent that a flat universe, together with the validity of GR ($\Omega_k = 0$, $\gamma = 1$), is strongly supported. More importantly, it is interesting to note that there exists a significant degeneracy between the spatial curvature of the universe and the PPN parameter, which captures how much space curvature is provided by the unit rest mass of the objects along or near the path of the particles. A similar degeneracy between γ and the other cosmological parameters (the matter density fraction, Ω_m , and the equation of state of dark energy, w) can also be seen from Figure 7.

One can easily check that reduction of the error of Ω_k would lead to more stringent fits of γ , which encourages us to consider

⁴ The assumption of 1% accuracy on the Einstein radius measurements from future LSST survey is reasonable, although the line-of-sight effect might introduce a $\sim 3\%$ uncertainty in the Einstein radii (Hilbert et al. 2009). However, according to the recent analysis by Collett & Cunningham (2016), the lines of sight for monitorable strong lenses (especially for quadruply imaged quasars) might be biased at the level of 1%. Some attempts to account for the line-of-sight secondary lensing for quasars can also be found in Collett et al. (2013), Greene et al. (2013), and Rusu et al. (2016).

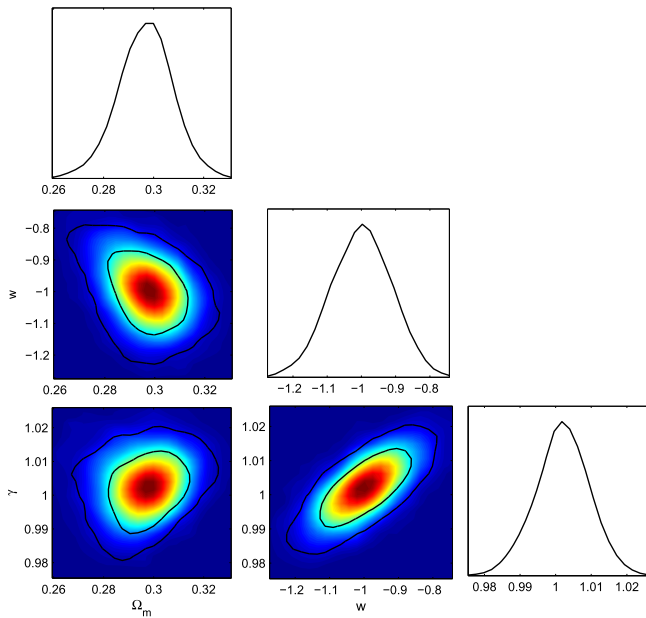


Figure 7. Constraints on the PPN parameter and cosmological parameters from the simulated LSST strong lensing data.

the possibility of testing PPN at a much higher accuracy with future surveys of strong lensing systems. We now set a prior on the cosmic curvature with $-0.007 < \Omega_k < 0.006$, according to the latest CMB data and baryon acoustic oscillation data (Ade et al. 2014), and get a constraint on the PPN parameter, $\gamma = 1.000^{+0.0023}_{-0.0025}$. When we changed the fractional uncertainty of the Einstein radius to the level of 1% and the observed velocity dispersion to the level of 5%, the resulting constraint on the PPN parameter became $\gamma = 1.000^{+0.0009}_{-0.0011}$. The posterior probability density for γ is shown in Figure 8. From this plot it is evident that much more severe constraints would be achieved, and one can expect γ to be estimated with a $10^{-3} \sim 10^{-4}$ precision.

5. CONCLUSIONS

Based on a mass-selected galaxy-scale strong gravitational lenses from the SLACS, BELLS, LSD, and SL2S surveys and a well-motivated fiducial set of lens-galaxy parameters, we tested the weak-field metric on kiloparsec scales and found a constraint on the post-Newtonian parameter $\gamma = 0.995^{+0.037}_{-0.047}$ under the assumption of a flat universe from *Planck* observations. Therefore, it is in agreement with the general relativity value of $\gamma = 1$ with 4% accuracy. Considering systematic uncertainties in total mass-profile shape, velocity anisotropy, and light-profile shape, we estimate systematic errors to be $\sim 25\%$.

Furthermore, we illustrated what kind of result we could get using the future data from the forthcoming Large Synoptic Survey Telescope (LSST) survey (Collett 2015). We applied a cosmological model-independent method to study the degeneracy (Räsänen et al. 2015) between cosmic curvature and the parameterized post-Newtonian parameter γ . It is apparent that spatially flat universe with the conservation of GR ($\Omega_k = 0$, $\gamma = 1$) is strongly supported. Moreover, the reduced uncertainty of Ω_k leads to more stringent fits of γ . This opens up the possibility of testing PPN with a much higher accuracy using strong lensing systems discovered in future surveys. By setting a prior on the cosmic curvature with $-0.007 < \Omega_k < 0.006$,

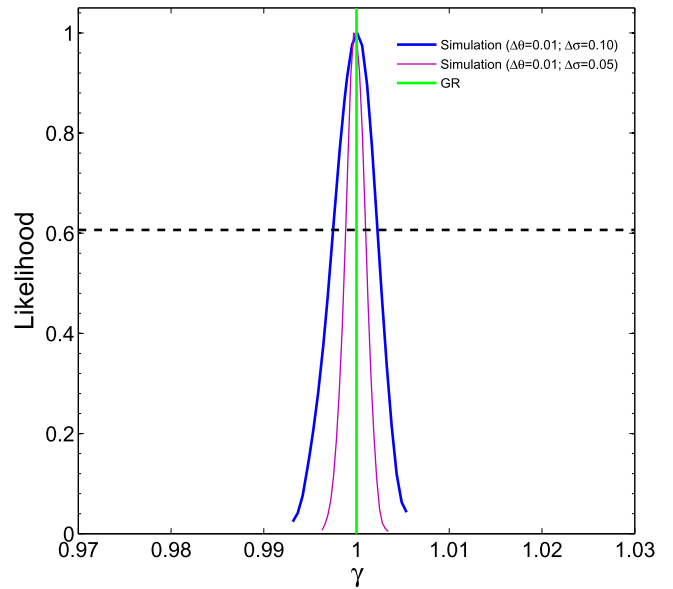


Figure 8. Constraints on the PPN parameter from simulated LSST strong lensing data, with a prior on the cosmic curvature $-0.007 < \Omega_k < 0.006$ from *Planck*.

assumed according to the latest CMB plus baryon acoustic oscillation data (Ade et al. 2014), the accuracy of γ determination reached a $10^{-3} \sim 10^{-4}$ precision.

We conclude that samples of strong lensing systems with measured stellar velocity dispersions, much larger than are currently available, may serve as an important probe to test the validity of GR, provided that mass-dynamical structure of lensing galaxies is better characterized and constrained in those future surveys.

This work was supported by the Ministry of Science and Technology National Basic Science Program (Project 973) under grant Nos. 2012CB821804 and 2014CB845806, the Strategic Priority Research Program “The Emergence of Cosmological Structure” of the Chinese Academy of Sciences (No. XDB09000000), the National Natural Science Foundation of China under grant Nos. 11503001, 11373014, and 11073005, the Fundamental Research Funds for the Central Universities and Scientific Research Foundation of Beijing Normal University, China Postdoctoral Science Foundation under grant No. 2015T80052, and the Opening Project of Key Laboratory of Computational Astrophysics, National Astronomical Observatories, Chinese Academy of Sciences. Part of the research was conducted within the scope of the HECOLS International Associated Laboratory, supported in part by the Polish NCN grant DEC-2013/08/M/ST9/00664—M.B. gratefully acknowledges this support. M.B. obtained approval of a foreign talent introduction project in China and gained special funds supporting this project.

REFERENCES

- Ade, P. A. R., Aghanim, N., Armitage-Caplan, C., et al. 2014, *A&A*, **571**, A16
Amanullah, R., Lidman, C., Rubin, D., et al. 2010, *ApJ*, **716**, 712
Ashby, N. 2002, *PhT*, **55**, 41
Auger, M. W., Treu, T., Bolton, A. S., et al. 2009, *ApJ*, **105**, 1099
Barnabè, M., Spiniello, C., Koopmans, L. V. E., et al. 2013, *MNRAS*, **436**, 253
Bernstein, G. 2006, *ApJ*, **637**, 598
Bertotti, B., Iess, L., & Tortora, P. 2003, *Natur*, **425**, 374
Biesiada, M. 2006, *PhRvD*, **73**, 023006

- Biesiada, M., Piórkowska, A., & Malec, B. 2010, *MNRAS*, **406**, 1055
- Binney, J. 1980, *MNRAS*, **190**, 873
- Bolton, A. S., Burles, S., Koopmans, L. V. E., et al. 2008, *ApJ*, **682**, 964
- Bolton, A. S., Rappaport, S., & Burles, S. 2006, *PhRvD*, **74**, 061501
- Bonvin, V., Courbin, F., Suyu, et al. 2016, arXiv:1607.01790
- Brownstein, J. R., Bolton, A. S., Schlegel, D. J., et al. 2012, *ApJ*, **744**, 41
- Cao, S., Biesiada, M., Gavazzi, R., Piórkowska, A., & Zhu, Z.-H. 2015a, *ApJ*, **806**, 185
- Cao, S., Biesiada, M., Yao, M., Zhu, Z.-H., et al. 2016, *MNRAS*, **461**, 2192
- Cao, S., Covone, G., Jullo, E., et al. 2015b, *AJ*, **149**, 3
- Cao, S., Covone, G., & Zhu, Z.-H. 2012a, *ApJ*, **755**, 31
- Cao, S., Pan, Y., Biesiada, M., Godlowski, W., & Zhu, Z.-H. 2012b, *JCAP*, **03**, 016
- Cao, S., & Zhu, Z.-H. 2012, *A&A*, **538**, A43
- Cao, S., & Zhu, Z.-H. 2014, *PhRvD*, **90**, 083006
- Cao, S., Zhu, Z.-H., & Zhao, R. 2012c, *PhRvD*, **84**, 023005
- Cardone, V. F., Piedipalumbo, E., & Scudellaro, P. 2016, *MNRAS*, **455**, 831
- Chae, K.-H. 2003, *MNRAS*, **346**, 746
- Chae, K.-H., Chen, G., Ratra, B., & Lee, D.-W. 2004, *ApJL*, **607**, L71
- Collett, T. E. 2015, arXiv:1507.02657
- Collett, T. E., & Auger, M. W. 2014, *MNRAS*, **443**, 969
- Collett, T. E., & Cunningham, S. D. 2016, *MNRAS*, **462**, 3255
- Collett, T. E., Marshall, P. J., & Auger, M. W. 2013, *MNRAS*, **432**, 679
- Dyson, F. W., Eddington, A. S., & Davidson, C. 1920, *RSPTA*, **220**, 291
- Gerhard, O., Kronawitter, A., Saglia, R. P., & Bender, R. 2001, *AJ*, **121**, 1936
- Golse, G., Kneib, J.-P., & Soucail, G. 2002, *A&A*, **387**, 788
- Greene, Z. S., Suyu, S. H., Treu, T., et al. 2013, *ApJ*, **768**, 39
- Grillo, C., Lombardi, M., & Bertin, G. 2008, *A&A*, **477**, 397
- Heymans, C., Van, W., Miller, L., et al. 2012, *MNRAS*, **427**, 146
- Hilbert, S., Hartlap, J., White, S. D. M., & Schneider, P. 2009, *A&A*, **499**, 31
- Hildebrandt, H., Choi, A., Heymans, C., et al. 2016, arXiv:1603.07722
- Jin, K.-J., Zhang, Y.-Z., & Zhu, Z.-H. 2000, *PhLA*, **264**, 335
- Keeton, C. R. 2001, *ApJ*, **561**, 46
- Koopmans, L. V. E. 2006, in EAS Publications Ser. 20, Mass Profiles & Shapes of Cosmological Structures, ed. G. A. Mamon et al. (Paris: EDP Sciences), 161
- Koopmans, L. V. E., & Treu, T. 2002, *ApJ*, **583**, 606
- Kuhlen, M., Keeton, C. R., & Madau, P. 2004, *ApJ*, **601**, 104
- MacCrann, N., Zuntz, J., Bridle, S., Jain, B., & Becker, M. R. 2015, *MNRAS*, **451**, 2877
- Mao, S. D., & Schneider, P. 1998, *MNRAS*, **295**, 587
- Marshall, P., Blandford, R., & Sako, M. 2005, *NAR*, **49**, 387
- Mitchell, J. L., Keeton, C. R., Frieman, J. A., & Sheth, R. K. 2005, *ApJ*, **622**, 81
- Ofek, E. O., Rix, H.-W., & Maoz, D. 2003, *MNRAS*, **343**, 639
- Oguri, M., Inada, N., Strauss, M. A., et al. 2008, *AJ*, **135**, 512
- Peebles, P. J. E. 1993, Principles of Physical Cosmology (Princeton, NJ: Princeton Univ. Press), 336
- Pound, R. V., & Rebka, G. A. 1960, *PhRvL*, **4**, 337
- Räsänen, S., Bolejko, K., & Finoguenov, A. 2015, *PhRvL*, **115**, 101301
- Riess, A. G., Macri, L. M., Hoffmann, S. L., et al. 2016, *ApJ*, **826**, 56
- Rusu, C. E., Fassnacht, C. D., Sluse, D., et al. 2016, arXiv:1607.01047
- Schneider, P., Ehlers, J., & Falco, E. E. 1992, Gravitational Lenses (New York: Springer)
- Schwab, J., Bolton, A. S., & Rappaport, S. A. 2010, *ApJ*, **708**, 750
- Shapiro, I. I. 1964, *PhRvL*, **13**, 789
- Sonnenfeld, A., Gavazzi, R., Suyu, S. H., Treu, T., & Marshall, P. J. 2013a, *ApJ*, **777**, 97
- Sonnenfeld, A., Treu, T., Gavazzi, R., et al. 2013b, *ApJ*, **777**, 98
- Suyu, S. H., Blandford, R. D., Fassnacht, C. D., et al. 2007, *BAAS*, **38**, 927
- Taylor, J. H., Fowler, L. A., & McCulloch, P. M. 1979, *Natur*, **277**, 437
- Thorne, K. S., & Will, C. M. 1971, *ApJ*, **163**, 595
- Treu, T., & Koopmans, L. V. E. 2002, *ApJ*, **575**, 87
- Treu, T., & Koopmans, L. V. E. 2004, *ApJ*, **611**, 739
- Treu, T., Koopmans, L. V., Bolton, A. S., Burles, S., & Moustakas, L. A. 2006, *ApJ*, **640**, 662
- Vegetti, S., Koopmans, L. V. E., Bolton, A., Treu, T., & Gavazzi, R. 2010, *MNRAS*, **408**, 1969
- Williams, J. G., Turyshev, S. G., & Boggs, D. H. 2004, *PhRvL*, **93**, 261101
- Wong, K. C., Suyu, S. H., & Matsushita, S. 2015, *ApJ*, **811**, 115
- Xu, D. D., Springel, V., Sluse, D., et al. 2016, arXiv:1610.07605v1
- Zhu, Z.-H. 2000a, *MPLA*, **15**, 1023
- Zhu, Z.-H. 2000b, *IJMPD*, **9**, 591
- Zhu, Z.-H., & Sereno, M. 2008, *A&A*, **487**, 831
- Zhu, Z.-H., & Wu, X.-P. 1997, *A&A*, **324**, 483
- Zhu, Z.-H., Hu, M., Alcaniz, J. S., & Liu, Y.-X. 2008, *A&A*, **483**, 15